Solid Freeform Fabrication 2021: Proceedings of the 32nd Annual International
Solid Freeform Fabrication Symposium – An Additive Manufacturing Conference
Reviewed Paper

Effect of process parameters on the vibration properties of PLA structure fabricated by additive manufacturing

Fangkai Xue[1,2], Guillaume Robin[1], Hakim Boudaoud[2], Fabio A. Cruz Sanchez[2], El Mostafa Daya[1]

1. Université de Lorraine, CNRS, Arts et Métiers ParisTech, LEM3, F-57000 Metz, France.
E-mail : fangkai.xue@univ-lorraine.fr
2. Université de Lorraine, Equipe de Recherche sur les Processus Innovatifs, ERPI, F-54000, Nancy, France.

Abstract

Advances in Fused Filament Fabrication (FFF) enable the design and manufacturing of multi-material and multi-functional structure that can potentially be used to develop light weight and high damping structures for vibration control. However, very few studies mention the vibration characteristics of FFF printed structures. This paper investigates the effect of four process parameters, raster angle, nozzle temperature, layer height and deposition speed, on the vibration properties of FFF printed Polylactic Acid (PLA) structure through modal analysis and design of experiment. The effects of all four parameters show a good agreement on the first fives modes of resonance. It was found that raster angle significantly affects both resonance frequency (16.6%) and loss factor (7.5%). Meanwhile, the impact of the other three parameters is relatively low (less than 4%), which is different from previous research results on static mechanical properties. All these results provide a guidance for further application of FFF in vibration field.

Keywords: Vibration properties, Fused Filament Fabrication (FFF), Modal Analysis, Polylactic acid (PLA), Design of Experiments (DoE)

A substantially improved version of this paper appears in a special issue of the TMS publication *JOM*, March 2022.

Introduction

Fused Filament Fabrication (FFF), also known as Fused Deposition Modeling (FDM) which is a trademark, is one of the most widespread Additive Manufacturing (AM) technologies. Although it is initially known as a low-cost rapid prototyping technology, nowadays FFF has become much more powerful due to various technical advancements in the last decades[1]. Plenty new materials have been developed for FFF such as metallic [2], ceramic[3], fiber-reinforced polymers[4], and bio-polymers [5]. Recent developments in hybrid FFF [6] and multi-material FFF [7] provide a much wider space for the design and manufacturing of multi-functional structures. At the structure level, the design novel metamaterials and architecture structures [8], [9] with customized material properties has been realized via FFF.

All these progresses enable the application of FFF in many fields, such as vibration control. Some preliminary attempts have already been done in the literature. Compton et al. [10] reported the extrusion-based 3D printing of cellular composites by a new epoxy-based ink with controlled

alignment of multi-scale, high aspect ratio fiber reinforcement. Matlack *et al.* [8] demonstrated the fabrication of a metamaterial for low-frequency and broadband vibration absorption with FFF printed lattice and manually inserted steel cube damper. Mizukami *et al*. [4] presented a FFF printed locally resonant carbon-fiber reinforced acoustic metamaterial for attenuation of broadband vibration.

Despite the research efforts, the application of FFF in the field of vibration control is still very few compared with its application in the other fields like static mechanical. As reported, the FFF process is controlled by many process parameters which have a large impact on the final parts' mechanical properties [11]–[14]. Thus, one of the biggest obstacles remains in the lack of research on the effect of process parameters on the vibration properties of FFF printed structures.

In the literature, large efforts have been made to discover the relationship between the process parameters and static mechanical properties of FFF printed parts, including tensile strength [11], flexural strength [13], fracture properties [14] and fatigue [15]. Rezayat et al. [16] reported that a raster angle along the direction of load resulted in higher tensile strength because the bonding of polymer between the adjacent filament is not as strong as bonding of polymer within the filament. Goh *et al.* [12] demonstrated that lager layer height and higher printing speed result in smaller degree of cooling and higher average temperature of the deposited filament, which can improve the interlayer fusion and results in higher mechanical properties in across-the-layer direction.

Concerning the vibration properties, although many studies mentioned the vibration characterization of FFF printed structures [14] [18] [19], very few articles aimed at finding the relation between the process parameters and the vibration properties of final parts. Seedhara *et al.* [20] investigated the effect of build orientation and layer height on the modal properties of FFF printed ABS beams. They reported that the increase of layer height declined the natural frequencies and the specimen printed in horizontal orientation had the highest natural frequencies. Raffic *et al.* [21] studied the effect of infill density, layer height and deposition speed on the natural frequency and resonant amplitude of FFF processed Polyethylene Terephthalate Glycol-modified (PET-G) and Acronitrile Butadiene Styrene (ABS) beams.

A comprehensive understanding of the effects of process parameters on the vibration properties of FFF fabricated parts is essential for further applications of FFF in vibration control. The purpose of this paper is to evaluate the performance of FFF in terms of vibration properties and characterize the effect of four process parameters, raster angle, nozzle temperature, layer height and deposition speed, on the vibration properties of FFF printed structures. Firstly, the reproducibility of the proposed protocol is evaluated in terms of the measured vibration properties of printed structures. Secondly, the effect of four key process parameters on the vibration properties of FFF printed PLA beams is investigated, where Design of Experience (DoE) and modal analysis are used. Finally, all these results provide a guidance for further application of FFF in vibration field.

Protocol of Investigation

In this section, the protocol of the investigation of the process parameters on the vibration properties of FFF printed PLA beams is presented.

Phase I: Set up of FFF and DoE

Material, machine and geometry

The material used is Polylactic Acid (PLA) (Raise Premium 1.75 mm PLA filament), which is the most used materials in FFF well known for its high rigidity, high strength, low melting point, non-toxic, non-irritation, and good biocompatibility [22]. PLA's high stiffness, good adaptability and operation simplicity enlarge its potential application in vibration control. The 3D printer used is a commercial dual extruder FDM machine Raise 3D E2. To investigate the flexural vibration modes, a beam specimen with a geometry of 3 mm thickness, 20 mm width and 200 mm length is chosen.

Parameters and their variation ranges for DoE

Four process parameters and one of their interactions are selected here as factors in design of experiment: raster angle (R); nozzle temperature (T); layer height (H); deposition speed (V); interaction between raster angle and nozzle temperature (R-T). In the literature, raster angle has a severe effect on the mechanical resistance of printed structure because of the anisotropy nature of FFF process [11]. The nozzle temperature, layer height and print speed control the thermal history of printing which dominants the bonding strength between filaments [12]. According to previous research, PLA has a high anisotropic property induced by the nature of the deposition process which makes the bond strength between filaments much weaker than the strength of deposed filaments [23]. The raster angle can change the orientation of structure anisotropy by arranging the direction of adjacent filament bonding. Meanwhile, the nozzle temperature influences the thermal history of printing and eventually control the filament bonding strength. Therefore, it's supposed that there is an interaction between the raster angle and the nozzle temperature on the vibration properties of FFF structures.

The limit values of parameters were determined through a preliminary test as shown in Table 1. Nozzle temperature, layer height and deposition speed have three levels. To study the effect of interaction between the raster angle and the nozzle temperature, a Taguchi $L18(2^1 3^3)$ orthogonal array was developed in the next section. Thus, the raster angle only has two levels due to statistical limitation of DOE method. To obtain the maximum difference in stiffness and verify the maximum effect of parameters, 90° and 0° were chosen as raster angles. Values of other process parameters are presented in Table 2.

Table 1 Levels of factors for Taguchi design of experiment of PLA

Levels	R (°)	T (°C)	H (mm)	V (mm/S)
1	0	190	0.1	20
2	90	220	0.2	55
3	/	250	0.3	90

Table 2 Fixed Process parameters

Parameter	**Value**
Build orientation	Horizontal
Extrude width	0.4mm
Flowrate	100%
Bed temperature	60°C
Cooling	100%
Shell	0
Infill density	100%
Infill pattern	Line

Design of experiment in use of Taguchi method

Taguchi method is selected for the design of experiment because of its good balance between statistical analysis and operation simplicity [24]. A Taguchi $L18(2^1 3^3)$ orthogonal array is selected to evaluate the effect of these 5 factors. R has two levels, while T, H and V have three factor levels.

Table 3 Taguchi $L18(2^1 3^3)$ Orthogonal Arrays for the DoE of PLA

Trials	Specimen	Replication	Factors				
			R	T	H	V	R-T
1	PLA 1111	2	1	1	1	1	
2	PLA 1122	2	1	1	2	2	(1,1)
3	PLA 1133	2	1	1	3	3	
4	PLA 1211	2	1	2	1	1	
5	PLA 1222	2	1	2	2	2	(1,2)
6	PLA 1233	2	1	2	3	3	
7	PLA 1312	2	1	3	1	2	
8	PLA 1323	2	1	3	2	3	(1,3)
9	PLA 1331	2	1	3	3	1	
10	PLA 2113	2	2	1	1	3	
11	PLA 2121	2	2	1	2	1	(2,1)
12	PLA 2132	2	2	1	3	2	
13	PLA 2212	2	2	2	1	2	
14	PLA 2223	2	2	2	2	3	(2,2)
15	PLA 2231	2	2	2	3	1	
16	PLA 2313	2	2	3	1	3	
17	PLA 2321	2	2	3	2	1	(2,3)
18	PLA 2332	2	2	3	3	2	

Phase II: experiment

Vibration test setup: modal analysis

Modal analysis is used to characterize the vibration properties of PLA beams. Figure 1 shows the experimental setup for measuring the frequency response curves of beams in forced vibration.

The shaker generates vibrations that were controlled and measured by a controller device (UCON system). The range of frequency excitation is between 10 and 2000 Hz. The vibration amplitude of the shaker was controlled using an accelerometer (PCB Piezotronics). The amplitude of the shaker was chosen to minimize nonlinear vibrations typically 1 mm displacement between 10 and 2000 Hz and a 1g acceleration between 10 and 1500 Hz. The amplitude of the beam's vibration was measured by a laser vibrometer. The response spectrum using FRF (Frequency Response Function) data was used to determine the resonant frequencies and the loss factors which was calculated by the Half Power Bandwidth Method (HPBM, also known as-3dB method) [25].

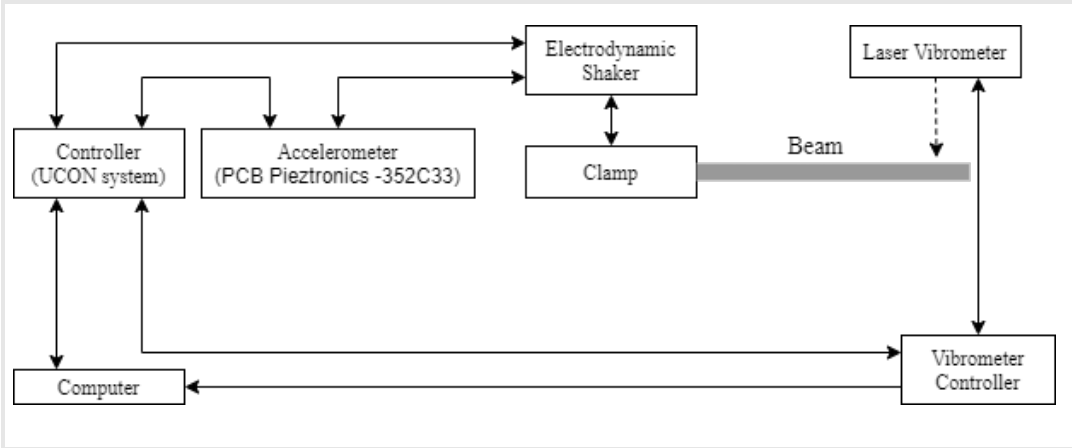

Figure 1 Experiment setup of modal analysis

For PLA specimens, the boundary condition is clamped-free and the laser spot was pointed on the free extremity of the beam which can capture all vibration mode on the selected spectral. The beams were attached to the shaker by an apparatus with a clamp length of 15 mm.

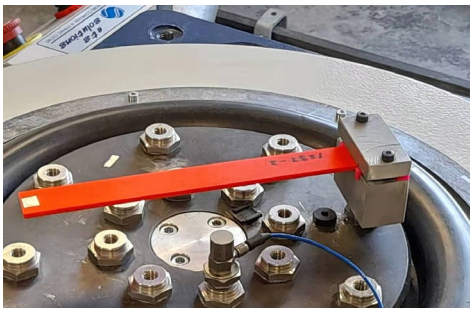

Figure 2 Boundary condition of modal analysis. Clamped-Free

Measured vibration properties

To establish a quantitative qualification, two vibration properties were selected as key factors: the resonant frequency and the loss factors. Resonant frequency is a fundamental index of vibration in frequency domain vibration test [25]. Moreover, the damping of structures is very important for vibration control. And loss factor is a common index used to characterize the damping of material or structure, which is equal to the ratio between the loss modulus and the storage modulus [26].

Result and Discussion

Reproducibility evaluation of the proposed protocol

To guarantee the reliability of the identified parameters effect, the precision of the FFF process and the vibration test prototype was evaluated in terms of the reproducibility of the measured vibration properties. PLA beams with a geometry of 3 mm thick, 20 mm large and 200 mm long were printed six times repetitively, using medium parameter levels as follows: R, 0°, T, 220°C; H, 0.2 mm; V, 55 mm/s.

As shown in table 4, percentage error is the ratio between the standard deviation and the average value. The results of resonant frequencies show a high-level reproducibility with a percentage error smaller than 1%. On the other hand, the percentage errors of loss factors are much higher than those of resonant frequencies, but still good (smaller than 6%). That is because the damping of PLA is relatively low. Therefore, the value of loss factors is too small to be precisely measured.

Table 4 Reproducibility of FDM printed PLA beam.

Item	Mode 1	Mode 2	Mode 3	Mode 4	Mode 5
Resonant Frequency (Hz)	21.97±0.12	135.77±1.02	379.52±2.45	744.56±4.77	1228.84±8.12
Percentage error (%)	0.57	0.75	0.65	0.65	0.67
Loss Factor	0.0292±3.65E-04	0.0149±8.18E-04	0.0125±6.91E-04	0.0122±6.53E-04	0.0127±6.31E-04
Percentage error (%)	1.26	5.86	5.78	5.56	5.13

With low level deviation and percentage error, the reproducibility of fabrication and modal analysis is verified within the selected process parameter level. The reproducibility may vary with the changes of process parameter, but this variation is the influence of process parameter itself but not the effect of machine calibration nor the effect of experiment setup.

Main effects on the resonant frequency of PLA beams

Through modal analysis, five resonant modes of PLA beam are obtained. The mains effects of parameters on PLA are presented in Figure 3, 4 and 5. Since the resonant frequency of each mode varies from 20 to 1500 Hz, the mains effects of parameters are normalized by the average resonant frequency of all specimens in each mode to make a comparable analysis. Similarly, main effects of loss factors are normalized by the average loss factor of all specimens in each mode.

Although the effects of the other three parameters are relatively low (below 3%) compared with the effect of raster angle (about 16%). These effects show a consistent trend

across all five resonant modes.

Considering raster angle in Figure 3 (a), from 90° to 0°, the resonant frequencies decrease by 16.6%. This shows that PLA has high anisotropic property in terms of resonant frequency, which is consistent to the reported anisotropy [27], [28] in static mechanical properties. A raster angle perpendicular to the axe of vibration form (axial axe for flexural vibration mode) leads to a larger resonant frequency as well as higher stiffness.

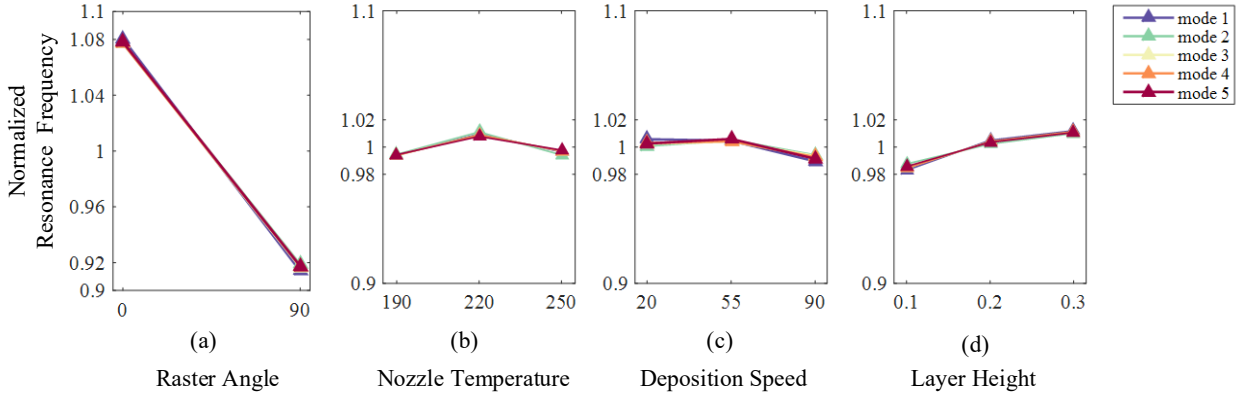

Figure 3 Effect of process parameters on the resonant frequencies of PLA beam

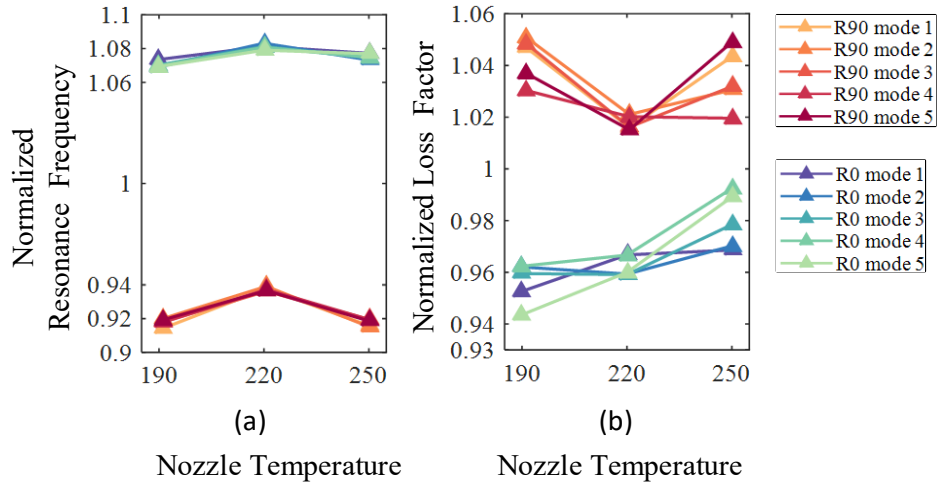

Figure 4 Effect of interaction between the raster angle and the nozzle temperature on the vibration properties of PLA beam

Nozzle temperature shows a nonlinear behavior in Figure 3 (b), where the resonant frequency increases by 1.6% from 190 °C to 220 °C, then decreases by 1.3% from 220°C to 250°C. The increase of resonant frequency from low temperature to middle temperature can be explained by the improve of bonding degree between filaments. As reported by Goh *et al.* [12], a higher average temperature leads to better bonding strength. The reason of the decrease

of resonant frequency from middle temperature to high temperature is believed to be radical degradation [22], where the high temperature level (250°C) is 80°C higher than the melting temperature of PLA [29].

Resonant frequency increases with the increase of layer height as shown in Figure 3 (c). From 0.1mm to 0.2 mm, resonant frequency increases by 2.2%; from 0.2 mm to 0.3 mm, resonant frequency increases by 0.7%. As layer height increases, fewer number of layers need to be deposed, resulting in fewer thermal cycles and smaller thermal gradient during printing, which was reported to have a positive effect on adhesion strength between filaments [12], thus leads to higher stiffness and higher resonant frequency.

For deposition speed, as shown in Figure 3 (d), the resonant frequency remains in the same level (0.7% of variation) as the deposition speed increase from 20 mm/s to 55 mm/s, and decreases by 1.5% as deposition speed increase from 55 mm/s to 90 mm/s. Higher deposition speed leads to fewer time for bonding formation between filaments and smaller necks.

The effect of interaction between raster angle and layer height is shown in Figure 4. The effect of nozzle temperature shows same trends on all levels of layer height but is more important at higher level of raster angle. At 0°, resonant frequency increases by 0.8% as nozzle temperature increases from 190 °C to 220°C then decreases by 0.4% as nozzle temperature increases from 220 °C to 250°C. This effect is very weak which is at the same level of measurement deviation assessed in reproducibility test. At 90°, resonant frequency increases by 2.3% as nozzle temperature increases from 190 °C to 220°C then decreases by 2.2% as nozzle temperature increases from 220 °C to 250°C, which is more significant than effect of nozzle temperature at 0°. That's because the vibration of beam is in flexural mode. Thus, at 90°, the direction of filament bond is parallel to the axe of flexural mode and contributes more to the global flexural modulus of beam. This interaction shows that filament bond strength plays a more important role in vibration when the raster angle is parallel to the axe of vibration mode.

For the resonant frequencies of PLA beam, the following insights were retrieved:

- Raster angle has the most significant effect on the resonant frequency of PLA beam;
- Effects of nozzle temperature, layer height and deposition speed are relatively low;
- Effects of parameters show a consistency impact on all five resonant modes.

Main effects on the loss factors of PLA beams

Since the variation of loss factor for each mode is very similar, the following quantitative descriptions will be based on the first resonant mode. As shown in Figure 5 (a), raster angle has the most significant influence on the loss factor of PLA beams. From 0° to 90°, loss factors reduce by 7.5%. Considering nozzle temperature, loss factor drops by 0.7% from 190°C to 220°C and

increases by 1.4% from 220°C to 250°C. For deposition speed, loss factor increases by 0.8% from 20mm/s to 50mm/s, then increases by 1.4% from 55mm/s to 90mm/s.

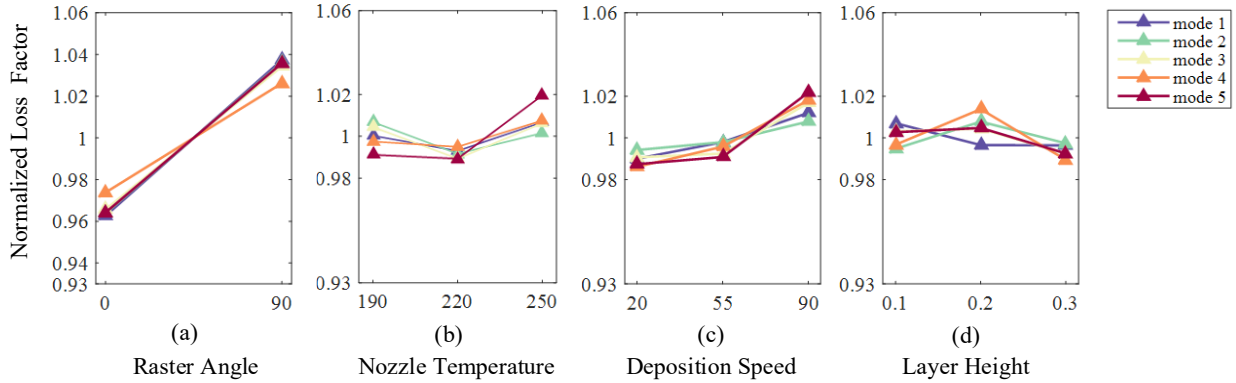

Figure 5 Effect of process parameters on the loss factors of PLA beam

For the loss factors of PLA beam, the following insights are retrieved:

- Values of loss factors are very small which indicates that the damping capacity of PLA beams is very low;
- Raster angle has a significant effect on the resonant frequency of PLA beam, while effect of nozzle temperature, layer height, raster angle is relatively weak;
- Except layer height, parameters shown consistency impact on all five resonant modes;
- Except for the layer height, effect of each parameter on the loss factors shows an inverse trend to its effect on the resonant frequencies.

Analysis of Variance

In order to provide a correct interpretation of the effect of factors, an ANOVA analysis is necessary. This provides significance rating of the relative influence of each factor analyzed in this study. Percentage contributions of each parameter on the response of specimens are also calculated.

Since the results of ANOVA are consistent for all the five resonant modes of PLA beam, only the result of the first mode, which is the most important for vibration control, is presented. Considering the effect on resonant frequency (contribution: 89.34%), result of ANOVA shows that raster angle is the most significant parameter, followed by layer height (Table 5).

Table 5 Significance of parameters on the resonant frequency of PLA beam

Source	Sum Sq.	d.f.	Mean Sq.	F	Prob>F	Signif	Contribution (%)
R	116.07	1	116.07	365.80	7.74E-17	***	89.34
T	0.90	2	0.45	1.42	0.26		0.21
H	2.97	2	1.49	4.68	0.02	*	1.80
V	1.06	2	0.53	1.67	0.21		0.33
R*T	0.31	2	0.16	0.49	0.62		-0.25
Error	8.25	26	0.32				8.57
Total	129.56	35					100.00
Signif. codes : 0 <'***'< 0.001< '**' <0.01 <'*' <0.05							

Considering the effect on the loss factor (Table 6), the raster angle is the only significant parameter, but it should be noted that there are large residual errors (contribution: 40.17%). There can be two sources for this residual error: (1) variable process parameters not considered in fabrication; (2) noisy of measurement in modal analysis. If the main cause is the first one, the residual errors for the resonant frequency should have a similar value compared to that of loss factor, which is not the fact. Therefore, this unusual residual error is mainly caused by the noisy measurement of loss factors in modal analysis because small value of loss factors makes the noise of measurement much more important.

Table 6 Significance of parameters on the loss factor of PLA beam

Source	Sum Sq.	d.f.	Mean Sq.	F	Prob>F	Signif	Contribution (%)
R	4.20E-05	1	4.20E-05	52.97	9.93E-08	***	59.66
T	9.44E-07	2	4.72E-07	0.59	0.56		-0.93
H	7.45E-07	2	3.72E-07	0.47	0.63		-1.22
V	2.49E-06	2	1.24E-06	1.57	0.23		1.30
R*T	2.29E-06	2	1.14E-06	1.44	0.25		1.01
Error	2.06E-05	26	7.93E-07				40.17
Total	6.91E-05	35					100.00
Signif. codes : 0 <'***'< 0.001< '**' <0.01 <'*' <0.05							

Conclusion and Perspective

In this study, the effect of four process parameters, raster angle, nozzle temperature, layer height and deposition speed, on the vibration properties of FFF printed PLA beams are investigated in use of modal analysis and DoE. It's found that FFF printed PLA beams have high resonant frequencies and small loss factors, which reflects its high stiffness and weak damping. A high reproducibility (percentage errors smaller than 1%) is also obtained in terms of resonant frequency in selected parameter level. Therefore, PLA is more suitable to be used as a rigid material to reinforce the stiffness of structures to prevent vibration other than a damping material to dissipate vibration energy. Follow guidelines are presented for the future design and manufacturing to

optimize the resonant frequency of PLA based FFF printed structures:

1. Raster angle has the largest effect on both resonant frequency (16.6% of variation) and loss factors (7.5% of variation). A raster angle perpendicular to the axe of vibration form (axial axe for flexural vibration mode) leads to a higher stiffness as well as higher resonant frequency.

2. The effect of layer height on the resonant frequency is much smaller than that of raster angle but still significant. Larger layer height leads to higher resonant frequency as the adhesion strength between filaments is improved by the reduction of thermal cycles and thermal gradient.

3. The effects of nozzle temperature, deposition speed and the interaction between raster angle and nozzle temperature on the resonant frequency are also observed in the experiment but not statistically significant. Therefore, a constant manufacturing quality can be achieved with in the selected range of nozzle temperature and deposition speed in terms of vibration properties.

It should be mentioned that the importance and influence of process parameters of different materials may be different. Therefore, future research should focus on materials different from PLA, such as elastomers, ceramics, and metals. The reproducibility of FFF process in terms of vibration properties should also be verified on different materials and geometries. Then a more universal guidance can be established to promote the further applications of FFF process in the manufacturing structures with complex geometry and multiple materials for vibration control.

Acknowledgements

The French Ministry of Research (DRRT), the regional Council "Région Lorraine", the European Regional Development Fund (FEDER) has contributed to the funding of the vibration and wave propagation platform. Also, the authors would like to thank to the research platform Lorraine Fab Living Lab® for the technical assistance in this research.

References

[1] S. Singh, G. Singh, C. Prakash, and S. Ramakrishna, "Current status and future directions of fused filament fabrication," *J. Manuf. Process.*, vol. 55, pp. 288–306, Jul. 2020, doi: 10.1016/j.jmapro.2020.04.049.

[2] S. H. Masood and W. Q. Song, "Thermal characteristics of a new metal/polymer material for FDM rapid prototyping process," *Assem. Autom.*, vol. 25, no. 4, pp. 309–315, Jan. 2005, doi: 10.1108/01445150510626451.

[3] S. Singh, S. Ramakrishna, and R. Singh, "Material issues in additive manufacturing: A review," *J. Manuf. Process.*, vol. 25, pp. 185–200, Jan. 2017, doi: 10.1016/j.jmapro.2016.11.006.

[4] K. Mizukami, T. Kawaguchi, K. Ogi, and Y. Koga, “Three-dimensional printing of locally resonant carbon-fiber composite metastructures for attenuation of broadband vibration,” *Compos. Struct.*, vol. 255, p. 112949, Jan. 2021, doi: 10.1016/j.compstruct.2020.112949.
[5] H. Chim *et al.*, “A comparative analysis of scaffold material modifications for load-bearing applications in bone tissue engineering,” *Int. J. Oral Maxillofac. Surg.*, vol. 35, no. 10, pp. 928–934, Oct. 2006, doi: 10.1016/j.ijom.2006.03.024.
[6] D. Grguraš and D. Kramar, “Optimization of Hybrid Manufacturing for Surface Quality, Material Consumption and Productivity Improvement,” *Stroj. Vestn. - J. Mech. Eng.*, vol. 63, pp. 567–576, Oct. 2017, doi: 10.5545/sv-jme.2017.4396.
[7] D. Espalin, J. Alberto Ramirez, F. Medina, and R. Wicker, “Multi-material, multi-technology FDM: exploring build process variations,” *Rapid Prototyp. J.*, vol. 20, no. 3, pp. 236–244, Jan. 2014, doi: 10.1108/RPJ-12-2012-0112.
[8] K. H. Matlack, A. Bauhofer, S. Krödel, A. Palermo, and C. Daraio, “Composite 3D-printed metastructures for low-frequency and broadband vibration absorption,” *Proc. Natl. Acad. Sci.*, vol. 113, no. 30, pp. 8386–8390, Jul. 2016, doi: 10.1073/pnas.1600171113.
[9] T. Jiang, C. Li, Q. He, and Z.-K. Peng, “Randomized resonant metamaterials for single-sensor identification of elastic vibrations,” *Nat. Commun.*, vol. 11, no. 1, Art. no. 1, May 2020, doi: 10.1038/s41467-020-15950-1.
[10] B. G. Compton and J. A. Lewis, “3D-Printing of Lightweight Cellular Composites,” *Adv. Mater.*, vol. 26, no. 34, pp. 5930–5935, 2014, doi: https://doi.org/10.1002/adma.201401804.
[11] T. J. Gordelier, P. R. Thies, L. Turner, and L. Johanning, “Optimising the FDM additive manufacturing process to achieve maximum tensile strength: a state-of-the-art review,” *Rapid Prototyp. J.*, vol. 25, no. 6, p. 19, 2019.
[12] G. D. Goh, Y. L. Yap, H. K. J. Tan, S. L. Sing, G. L. Goh, and W. Y. Yeong, “Process–Structure–Properties in Polymer Additive Manufacturing via Material Extrusion: A Review,” *Crit. Rev. Solid State Mater. Sci.*, vol. 45, no. 2, pp. 113–133, Mar. 2020, doi: 10.1080/10408436.2018.1549977.
[13] O. Luzanin, V. Guduric, I. Ristic, and S. Muhic, “Investigating impact of five build parameters on the maximum flexural force in FDM specimens – a definitive screening design approach,” *Rapid Prototyp. J.*, vol. 23, no. 6, pp. 1088–1098, Jan. 2017, doi: 10.1108/RPJ-09-2015-0116.
[14] N. Suksangpanya, N. A. Yaraghi, R. B. Pipes, D. Kisailus, and P. Zavattieri, “Crack twisting and toughening strategies in Bouligand architectures,” *Int. J. Solids Struct.*, vol. 150, pp. 83–106, Oct. 2018, doi: 10.1016/j.ijsolstr.2018.06.004.
[15] V. Shanmugam *et al.*, “Fatigue behaviour of FDM-3D printed polymers, polymeric composites and architected cellular materials,” *Int. J. Fatigue*, vol. 143, p. 106007, Feb. 2021, doi: 10.1016/j.ijfatigue.2020.106007.
[16] H. Rezayat, W. Zhou, A. Siriruk, D. Penumadu, and S. S. Babu, “Structure–mechanical property relationship in fused deposition modelling,” *Mater. Sci. Technol.*, vol. 31, no. 8, pp. 895–903, Jun. 2015, doi: 10.1179/1743284715Y.0000000010.

[17] R. Rajpal, L. K.P, and K. V. Gangadharan, “Parametric studies on bending stiffness and damping ratio of Sandwich structures,” *Addit. Manuf.*, vol. 22, pp. 583–591, Aug. 2018, doi: 10.1016/j.addma.2018.05.039.
[18] M. Mansour, K. Tsongas, and D. Tzetzis, “Measurement of the mechanical and dynamic properties of 3D printed polylactic acid reinforced with graphene,” *Polym.-Plast. Technol. Mater.*, vol. 58, no. 11, pp. 1234–1244, Jul. 2019, doi: 10.1080/03602559.2018.1542730.
[19] R. Rajpal, K. P. Lijesh, and K. V. Gangadharan, “Experimental investigation of 3D-printed polymer-based MR sandwich beam under discretized magnetic field,” *J. Braz. Soc. Mech. Sci. Eng.*, vol. 40, no. 12, p. 569, Dec. 2018, doi: 10.1007/s40430-018-1488-7.
[20] K. Sreedhara, K. Reddy, and S. N. S. H. Ch, “Vibration Properties of 3D Printed/Rapid Prototype Parts,” *Int. J. Innov. Res. Sci. Eng. Technol.*, vol. 3297, p. 4602, Jun. 2015, doi: 10.15680/IJIRSET.2015.0406087.
[21] N. M. Raffic, “EFFECT OF FDM PROCESS PARAMETERS ON VIBRATION PROPERTIES OF PET-G AND ABS PLASTICS,” *Int. J. Mech. Prod. Eng.*, vol. 3, no. 1, pp. 28–38, 2017.
[22] F. Carrasco, P. Pagès, J. Gámez-Pérez, O. O. Santana, and M. L. Maspoch, “Processing of poly(lactic acid): Characterization of chemical structure, thermal stability and mechanical properties,” *Polym. Degrad. Stab.*, vol. 95, no. 2, pp. 116–125, Feb. 2010, doi: 10.1016/j.polymdegradstab.2009.11.045.
[23] S. H. Ahn, C. Baek, S. Lee, and I. S. Ahn, “Anisotropic Tensile Failure Model of Rapid Prototyping Parts - Fused Deposition Modeling (FDM),” *Int. J. Mod. Phys. B*, vol. 17, no. 08n09, pp. 1510–1516, Apr. 2003, doi: 10.1142/S0217979203019241.
[24] N. Logothetis, “A perspective on Shainin’s approach to experimental design for quality improvement,” *Qual. Reliab. Eng. Int.*, vol. 6, no. 3, pp. 195–202, 1990, doi: https://doi.org/10.1002/qre.4680060306.
[25] M. F. Treszkai, B. Vehovszky, and D. Feszty, “Damping determination by the half power bandwidth method for a rectangular flat plate with bitumen damping layer application,” *J. Vibroengineering*, vol. 23, no. 5, Art. no. 5, 2021, doi: 10.21595/jve.2021.21938.
[26] K. Holeczek, P. Kostka, and N. Modler, “Dry Friction Contribution to Damage-Caused Increase of Damping in Fiber-Reinforced Polymer-Based Composites,” *Adv. Eng. Mater.*, vol. 16, no. 10, pp. 1284–1292, 2014, doi: 10.1002/adem.201400293.
[27] S.-H. Ahn, M. Montero, D. Odell, S. Roundy, and P. K. Wright, “Anisotropic material properties of fused deposition modeling ABS,” p. 11.
[28] C. Ziemian, M. Sharma, and S. Ziemi, “Anisotropic Mechanical Properties of ABS Parts Fabricated by Fused Deposition Modelling,” in *Mechanical Engineering*, M. Gokcek, Ed. InTech, 2012. doi: 10.5772/34233.
[29] “Properties of Raise 3D Premium 1.75 mm PLA filament.” https://s1.raise3d.com/2020/04/Raise3D-Premium-PLA_SDS_V4.pdf (accessed Jun. 20, 2021).